

Bottomonium from NRQCD with Dynamical Wilson Fermions ^{*}

SESAM - Collaboration:

A. Spitz^a, N. Eicker^a, J. Fingberg^b, S. Güsken^b, H. Hoerber^b, Th. Lippert^a, K. Schilling^{a,b}, J. Viehoff^b.

^aHLRZ c/o Forschungszentrum Jülich, D-52425 Jülich, and DESY, D-22603 Hamburg, Germany,

^bPhysics Department, University of Wuppertal, D-42097 Wuppertal, Germany.

We present results for the $b\bar{b}$ spectrum obtained using an $\mathcal{O}(M_b v^6)$ -correct non-relativistic lattice QCD action. Propagators are evaluated on SESAM's three sets of dynamical gauge configurations generated with two flavours of Wilson fermions at $\beta = 5.6$. Compared to a quenched simulation at equivalent lattice spacing we find better agreement of our dynamical data with experimental results in the spin-independent sector but observe no unquenching effects in hyperfine-splittings. To pin down the systematic errors we have also compared quenched results in different "tadpole" schemes and used a lower order action.

1. INTRODUCTION

Lattice NRQCD has been widely used in the past few years to calculate a variety of phenomenologically interesting quantities. The first step in the NRQCD program, naturally, is the calculation of the spectrum of the $b\bar{b}$ system. In the simulation presented here we use SESAM's large sample of dynamical Wilson-fermion gauge configurations to study both the spin-independent as well as the spin-dependent spectrum of the Υ . Our strategy, in searching for sea-quark effects, will be to compare our final dynamical results to that of a quenched simulation at equivalent lattice spacing. With our three sea-quark masses we can also study the dependence of mass-splittings on the light sea-quark mass. Recent simulations have exposed the sensitivity of spin-independent splittings to the details of the action. Therefore, in the spirit of [1,2], we have implemented the NRQCD action including spin-dependent corrections of $\mathcal{O}(M_b v^6)$ and we tadpole improve using the mean link calculated in Landau gauge. With these ingredients we hope to clarify the effect of unquenching in the spin-dependent splittings. In addition, using the quenched configurations we investigate: (i) the effect of changing tadpole prescriptions; (ii) the effect of using an $\mathcal{O}(M_b v^4)$ correct action compared to the $\mathcal{O}(M_b v^6)$ corrected one.

^{*}Talk presented by A. Spitz.

2. SIMULATION DETAILS

2.1. Action

The non-relativistic (Euclidean) lattice Hamiltonian to $\mathcal{O}(M_b v^6)$ consists of [3]: the kinetic energy operator,

$$H_0 = -\frac{\Delta^{(2)}}{2M_b}, \quad (1)$$

which is of order $M_b v^2$; relativistic corrections of order $M_b v^4$,

$$\begin{aligned} \delta H^{(4)} = & -c_1 \frac{(\Delta^{(2)})^2}{8M_b^3} + c_2 \frac{ig}{8M_b^2} (\Delta \cdot \mathbf{E} - \mathbf{E} \cdot \Delta) \\ & -c_3 \frac{g}{8M_b^2} \sigma \cdot (\tilde{\Delta} \times \tilde{\mathbf{E}} - \tilde{\mathbf{E}} \times \tilde{\Delta}) \\ & -c_4 \frac{g}{2M_b} \sigma \cdot \tilde{\mathbf{B}} \\ & +c_5 \frac{a^2 \Delta^{(4)}}{24M_b} - c_6 \frac{a (\Delta^{(2)})^2}{16nM_b^2}, \end{aligned} \quad (2)$$

and spin-sensitive corrections of order $M_b v^6$,

$$\begin{aligned} \delta H^{(6)} = & -c_7 \frac{g}{8M_b^3} \{\Delta^{(2)}, \sigma \cdot \mathbf{B}\} \\ & -c_8 \frac{3g}{64M_b^4} \{\Delta^{(2)}, \sigma \cdot (\Delta \times \mathbf{E} - \mathbf{E} \times \Delta)\} \\ & -c_9 \frac{ig^2}{8M_b^3} \sigma \cdot \mathbf{E} \times \mathbf{E}. \end{aligned} \quad (3)$$

The \mathbf{E} and \mathbf{B} fields are represented by the standard clover term or, where appropriate, by an im-

Table 1
Simulation details

$\beta_{\text{dyn}} = 5.6, n_f = 2, 16^3 \times 32$			
κ_{sea}	0.156	0.1570	0.1575
# configurations	200	200	200
measurements	800	800	800
$\beta_{\text{quenched}} = 6.0, n_f = 0, 16^3 \times 32$			
# configurations: 200			
measurements: 800			

proved version to remove $\mathcal{O}(a^2 M_b v^4)$ discretization errors. Following [4] the quark Greens functions are calculated from the evolution equation

$$G(t+1) = \left(1 - \frac{aH_0}{2n}\right)^n U_4^\dagger \left(1 - \frac{aH_0}{2n}\right)^n \times (1 - a\delta H) G(t), \quad (4)$$

$$G(0) = \delta_{\mathbf{x},0},$$

with $n = 2$ [3]. We rely on tapole improvement choosing the mean link in Landau gauge as our improvement scheme. The coefficients c_i are then set to their tree level value of 1.

2.2. Lattice Parameters

The lattice parameters we have used are displayed in table 1. Details concerning the generation of our dynamical configurations and issues surrounding autocorrelations are discussed in ref. [5]. We exploit configurations more than once by starting the propagator evolution both at different spatial source points and on different timeslices. A binning procedure confirms that our 4 measurements per configuration are indeed independent. Throughout, we fix the bare heavy quark mass to a value $aM_b = 1.7$.

3. SPECTROSCOPY

For details concerning the choice of operators, smearing techniques and fitting procedures we refer to [6]. We extrapolate energy level splittings linearly in the quark mass:

$$\Delta m = \Delta m_0 + c \sum_{u,d,s} m_q, \quad (5)$$

where m_q denotes the bare light quark masses (see figure 1 for an example). The relevant scale we

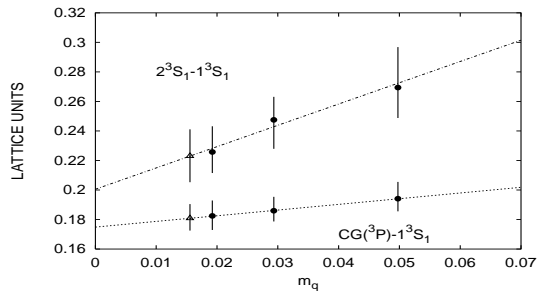


Figure 1. Extrapolation of spin independent splittings to $m_s/3$. The triangular symbol denotes the extrapolated value.

	Average $a^{-1}[\text{GeV}]$	R_{SP}
$n_f = 0, \beta = 6.0$	2.47(10)	1.43(9)
$\kappa = 0.1560$	2.18(12)	1.39(13)
$\kappa = 0.1570$	2.32(10)	1.33(12)
$\kappa = 0.1575$	2.45(12)	1.24(13)
$m_s/3$	2.48(14)	1.23(11)

Table 2

We use the average lattice spacing from the $2^3S_1 - 1^3S_1$ and $1^3P - 1^3S_1$ to convert our results to physical units. R_{SP} is to be compared to the experimental value of 1.28.

pick is given by $\frac{m_u + m_d + m_s}{3} \approx \frac{m_s}{3}$. The value of the strange quark mass is taken from our recent light quark mass calculation [7] and is such that $\frac{m_s}{3} \simeq 0.0156$ lies close to our lightest sea quark mass.

Figure 2 and 3 summarize our results for 2 and 0 flavours. Unquenching effects are clearly visible in the spin-independent part of the $b\bar{b}$ spectrum. This is also evident from table 2: $R_{SP} \equiv (2^3S_1 - 1^3S_1)/(1^3P - 1^3S_1)$ disagrees with the experimental value $R_{SP} = 1.28$ in the quenched case but coincides with it when dynamical fermions are included.

We do not observe any significant impact of unquenching on the hyperfine splittings. In particular, the P-hyperfine splittings seem to be underestimated for both $n_f = 0$ and $n_f = 2$. Clearly, this result needs to be corroborated with higher statistics. Errors on our hyperfine splittings encompass the statistical error as well as the uncertainty in the fitting range; the latter is essentially of the

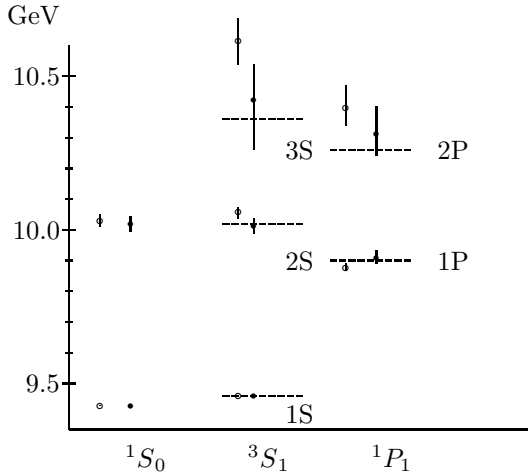


Figure 2. The $b\bar{b}$ spectrum: radial and angular momentum splittings with the Υ -level set to its physical value. Open circles : $n_f = 0, \beta = 6.0$; filled circles : $n_f = 2, m_q = m_s/3$; lines: experiment.

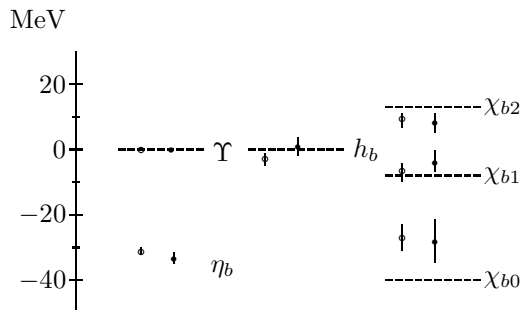


Figure 3. Fine structure: here the zero of energy is set to the Υ -level in the left part and to the spin averaged triplet P -level in the right part. Labels as in 2.

same size as the statistical error so that we can expect some improvement with higher statistics.

We expect the inclusion of $\mathcal{O}(M_b v^6)$ terms to effect the hyperfine splittings on the 10 % level, since $v^2 \approx 0.1$. Performing a relatively inexpensive $\mathcal{O}(M_b v^4)$ quenched simulation at $\beta = 6.0$ (with 200 measurements) we find this naive expectation to be well satisfied for the ${}^3S_1 - {}^1S_0$ splitting as is shown in figure 4. However, using the plaquette prescription for u_0 (result from the NRQCD-Collab., also included in figure 4) shifts the value on the 10% level in the opposite direc-

tion as adding $\mathcal{O}(M_b v^6)$ corrections.

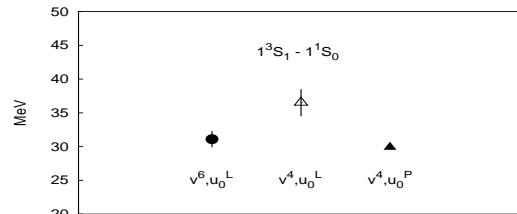


Figure 4. Hyperfine S-splitting obtained with an $\mathcal{O}(M_b v^6)$ and $\mathcal{O}(M_b v^4)$ correct NRQCD action. The higher order result is shifted significantly downward. Also shown: result with an $\mathcal{O}(M_b v^4)$ action but using the plaquette tadpole scheme. All results are for the quenched case with $\beta = 6.0$.

4. SUMMARY AND OUTLOOK

Overall, NRQCD has proven to work very well in the spin-independent sector, in particular in giving a precise determination of the lattice spacing a . It appears worthwhile to push the scale determinations to higher statistics using our configurations generated by T χ L at $\kappa = 0.1575$ on $24^3 \times 40$ lattices ($\beta = 5.6$). This would enable a reliable extrapolation to 3 or 4 flavours. The dominant source of error in such a lattice scale determination is most likely due to the remaining lattice discretisation errors in the gauge configurations.

Although higher statistics are highly desirable, it seems unlikely that progress in the spin-dependent sector will come from this approach alone. It is worrying to find the spin-dependent corrections of $\mathcal{O}(M_b v^6)$ as large as 10 % even for the $b\bar{b}$, decreasing the fine-splittings relative to the lower order estimates. A perturbative or non-perturbative calculation of the coefficients c_i is badly needed.

REFERENCES

1. H. D. Trottier, Phys. Rev. D**55**, 6844 (1997)
2. T. Manke *et al.*, hep-lat/9706003
3. G. P. Lepage *et al.*, Phys. Rev. D**46**, 4052 (1992).

4. C. T. H. Davies *et al.*, Phys. Rev. D**50**, 6963 (1994).
5. SESAM collaboration, hep-lat/9707004
6. SESAM collaboration, hep-lat/9709002
7. SESAM collaboration, hep-lat/9704019